INTERNATIONAL JOURNAL OF AGRICULTURE & BIOLOGY
ISSN Print: 1560–8530; ISSN Online: 1814–9596
23–0129/2023/30–2–129–138
DOI: 10.17957/IJAB/15.2067
http://www.fspublishers.org

Full Length Article

Effects of Zinc Oxide Nanoparticles on Mice Exposed to Methotrexate

Bakhsh Noor[1] , Saad Yasser Mohamed[1,2*], Rabah Samar[1] and Ahmad Mahmoud Saeed[3]
[1]*Department of Biological Sciences, Faculty of Sciences, King Abdulaziz University, Saudi Arabia*
[2]*Conservation of Biological Aquatic Resources Research Group, KAU, KSA*
[3]*Princess Dr. Najla Bint Saud Al-Saud Center for Excellence Research in Biotechnology, King Abdulaziz University, Jeddah, Saudi Arabia*
[*]For correspondence: yasser_saad19@yahoo.com
Received 22 April 2032; Accepted 06 July 2023; Published 10 August 2023

Abstract

Patients receiving Methotrexate (MTX) treatments commonly encounter numerous side effects. Zinc oxide nanoparticles have gained attention in various fields, including medicine, due to their potential applications in drug delivery, imaging and therapy. This investigation aimed to assess the effects of Zinc oxide nanoparticles on male mice exposed to Methotrexate via isozyme electrophoresis and Semi-Quantitative RT-PCR. Polyacrylamide electrophoresis was utilized to separate different isozyme systems, such as Malate dehydrogenase, Esterase, Superoxide dismutase, and Lactate dehydrogenase, in order to identify specific biochemical tags associated with the effects of Methotrexate (MTX) and/or Zinc Oxide nanoparticles (ZnONPs). The results showed that Zinc oxide nanoparticles and/or MTX can alter the intensity and/or the numbers of some isozyme bands in certain mice body organs. Isozyme systems have proven to be real tags of differential gene expression in some mice body organs (liver, kidney and spleen). The results showed Up-Regulation of the liver Sod gene expression under the experimental conditions. Further biological investigations are necessary to thoroughly evaluate the effects of Methotrexate (MTX) medications and effectively mitigate any potential side effects.

Keywords: Gene expression; Isozymes; Zinc oxide nanoparticles; Methotrexate

Introduction

Nanoparticles have exceptional properties (compared with other bulk chemicals) such as a high surface area to volume ratio and plentiful reactive sites on the surface. The application of Nanotechnology has been dramatically increasing in the past decade in many fields including cosmetics, paints, nutrient delivery, the medical field, the food industry and testing (Singh and Nalwa 2011; Kumar *et al.* 2013; Hong *et al.* 2015; Peters *et al.* 2016; Chen *et al.* 2020; Alamri *et al.* 2021; Elsebaie and Saad 2022).

About 1.2 million tons of ZnO-NPs are annually produced around the world (Scherzad *et al.* 2017).

Zinc oxide nanoparticles (ZnO NPs) have been found to have some positive impacts on mitochondrial enzymes in various studies. The potential positive impacts of this material include Enhancement mitochondrial function, increasing antioxidant capacity, Preservation of enzyme activity and promotion of mitochondrial biogenesis (Adegbeye *et al.* 2019). It's important to note that the effects of ZnO NPs on mitochondrial enzymes can vary depending on factors such as concentration, duration of exposure and specific experimental conditions.

The probable toxicity of the zinc oxide nanoparticles through the oral route was discussed in some studies (Pasupuleti *et al.* 2012; Mansouri *et al.* 2015; Muthuraman and Hwan 2015; Chen *et al.* 2020). The nanoparticles have enormous probable effects on biological responses. The ZnO-NPs could be dissolved in the stomach. Also, it could be absorbed into the systemic circulation. The probable toxicity effects of these materials under certain conditions were discussed in some investigations (Gojova *et al.* 2007; Lin *et al.* 2009; Pasupuleti *et al.* 2012; Cho *et al.* 2012; Mansouri *et al.* 2015).

Methotrexate (MTX) is broadly used in treatments of some cancer types, inflammations and rheumatoid. Determination of the effects of Methotrexate was carried out using different laboratory methods such as biochemical, cytogenetic and histological methods (Mansour *et al.* 2012; Schmidt *et al.* 2022). On the other hand, the physiological and/or biochemical genetic changes due to the ZnO-NPs effects in various biological systems are not saturated and still unclear (Abass *et al.* 2017).

Regarding Methotrexate, Patients receiving MTX treatments commonly encounter various side effects, including allergic reactions, skin discomfort, eye irritation, and intestinal mucus production. Several biological studies have provided evidence of the hepatotoxicity caused by Methotrexate treatments in mammals, demonstrating its effects at both histological and physiological levels.

However, the understanding of Methotrexate's genetic impact on various biological systems, including mammals, remains incomplete (Mansour *et al.* 2012; Schmidt *et al.* 2022).

By investigating the different isozymes including Esterase (break down and convert ester bonds in chemical compounds), Lactate dehydrogenase (converting lactate to pyruvate), Malate dehydrogenase (catalyze the conversion of malate to oxaloacetate), Super oxide dismutase (catalyzes the conversion of superoxide radicals into oxygen and hydrogen peroxide) and their distribution patterns, we can gain insights into tissue-specific metabolic activities (Mansour *et al.* 2012; Elsebaie and Saad 2022).

The accuracy and specificity of Semi-Quantitative reverse transcription polymerase chain reaction (sqRT-PCR) in measuring gene expression levels have been extensively discussed in numerous investigations (Wang 2021).

This study aimed to assess the effects of Zinc oxide nanoparticles on male mice exposed to MTX via isozyme electrophoresis and sqRT-PCR techniques.

Materials and Methods

The green synthesized ZnO-NPs (165.25 ±4.6nm) were obtained from the Conservation of biological aquatic resources research group, Biological Sciences Department, Faculty of Sciences, King Abdulaziz University.

Methotrexate (MTX) was purchased from the pharmacy (500 mg/20 mL).

Genetically pure male mice individuals (25.1± 5g) were housed as mentioned by Mansour *et al*. (2012) for acclimatization to the laboratory conditions.

MTX treatments and LD50 determination were carried out as described by Wheeler *et al*. (1995) and Mansour *et al.* (2012) with some modifications. MTX was intraperitoneally injected (20 mg/kg).

Mice (n=20) were divided equally into four groups (I, II. III and IV) as follows:

Group I: control; mice (n=5) were injected with saline (0.9% NaCl) intraperitoneally and kept as healthy control.

Group II: mice (n=5) were treated with MTX (20 mg/kg/I.P.) twice weekly on (Sunday and Thursday).

Group III: MTX + ZnO-NPs; mice (n=5) were administered oral gavage daily with (ZnO-NPs) and then treated with MTX (20 mg/kg/I.P.) twice weekly on (Sunday and Thursday).

Group IV: mice (n=5) were administered oral gavage daily with zinc oxide nanoparticles at a dose of 0.2 mg/kg body weight.

On day 40, the blood samples were withdrawn from each individual. Also, mice were killed, the liver, kidney and spleen organs were excised, weighed, frozen (Mansour *et al*. 2012) and kept at -80°C.

Isozyme extraction

Saline soluble Isozyme samples were extracted from three mice body organs (liver, kidney and spleen). Also, the serum samples were prepared for separation via polyacrylamide gel electrophoresis (Mansour *et al.* 2012).

Isozyme separation

Esterase (a-naphthyl acetate), Malate dehydrogenase (Mdh), Lactate dehydrogenase (Ldh) and Superoxide dismutase (SOD) isozyme systems were applied to differentiate biochemical differences among the control and treated samples.

Electrophoretic conditions, gel preparation, staining and distaining were carried out according to Pasteur *et al*. (1988), Mansour *et al.* (2012) and Elsebaie and saad (2022).

sqRT-PCR

The RNA samples were extracted from the liver tissue (100 mg) using TRIzol as described by Rio *et al.* (2010). The samples were quantitatively measured as described by Romero *et al.* (2007).

A sqRT-PCR method was applied to evaluate Sod gene expression under experimental conditions. The cDNA synthesis was carried out according to Meadus (2003).

As a control, B-actin gene fragments were amplified. The B Actine primer pairs were as follows: B-Actin_F: GGCACCACACCTTCTACAATG and B-Actin_R: GGGGTGTTGAAGGTCTCAAAC. The PCR reaction and condition were carried out according to Wei *et al.* (2014).

Concerning the Sod gene fragments, the primer pairs were as follows: Sod_F:TTTTTGCGCGGTCCTTTCCTG and Sod_R:GGTTCACCGCTTGCCTTCTGCT. The PCR reaction and condition were carried out according to Singh *et al*. (2012).

Data analysis

The isozyme gel banding patterns were analyzed as described by Elsebaie and Saad (2022). Concerning the B-Actin and Sod gene fragments, the bands were analyzed using the Gel Analyzer 19.1 software (WWW.gelanalyzer.com).

The statistical analysis involved conducting various sample test analyses of variance (ANOVA) to compare the values. A significance level of $P \leq 0.05$ was considered to determine statistical significance. The obtained results were statistically analyzed using Paleontological Statistics (PAST), Version 4.03 (https://past.en.lo4d.com/windows).

Results

Isozyme variations

The results revealed some variable mice tissue responses under certain conditions. All samples revealed patterns of anodally separated isozyme (Esterase, Malate dehydrogenase, Lactate dehydrogenase and Superoxide

Table 1: The resolution of each isozyme banding pattern for every extracted mouse sample type (Under the experimental conditions).

Tissue		Serum		Liver		Kidney		spleen	
System	En	resolution	NDB	resolution	NDB	resolution	NDB	resolution	NDB
Est	3.1.1.1	+++	14	+++	20	+++	20	++	10
Mdh	1.1.1.37	++	15	++	9	++	3	++	1
Ldh	1.1.1.27	+++	10	+++	3	+++	5	+++	6
Sod	1.15.1.1	+++	9	++	3	++	3	++	4

Est. = Esterase, Sod= Superoxide dismutase, Mdh = Malate dehydrogenase, Ldh = Lactate dehydrogenase, En= Enzyme number, +++ = strong, ++ = Moderate, + = Weak, - = No detectable reaction and NBD= Number of detected bands

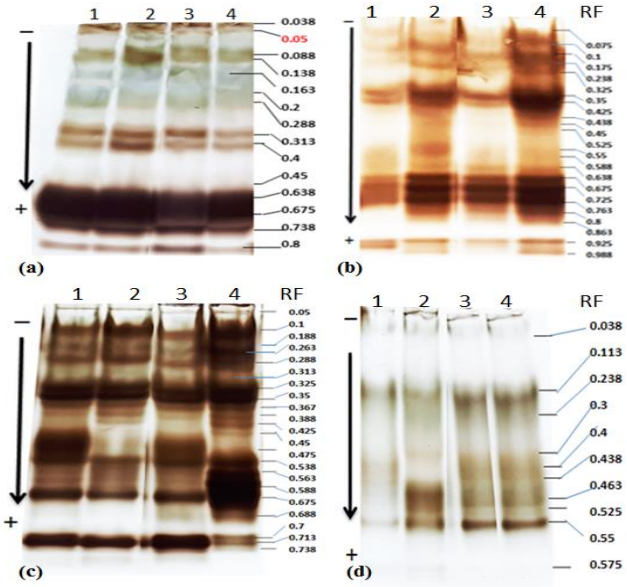

Fig. 1: The Esterase banding patterns from different samples. Serum (a), Liver (b), Kidney (c) and Spleen (d) tissues. 1= Control, 2= MTX, 3= MTX + ZnO-NPs and 4= ZnO-NPs

dismutase) bands (Figs. 1, 3, 5 and 7). The numbers of the detected bands were presented in Table (1 and 2).

Esterase variations

The electrophoretic profiles of the esterase isozymes (Fig. 1) in the evaluated samples (serum, liver, kidney and spleen) revealed notable bands. The separated esterase isozymes exhibited intense pattern in all the evaluated samples.

The resolution and the total characterized bands were summarized in Table (1). The numbers of the identified bands were adjustable among the evaluated organs. The averages of the band frequencies (ABF) were summarized in Table (2). The highest ABF (0.98) value was calculated in the serum esterase. On the other hand, the lowest (0.86) value was calculated for the Kidney esterase.

A total of 14 serum esterase bands (Fig. 1) were characterized (Rf ranged from 0.038 to 0.8). Only one serum esterase band (Rf= 0.05) was absent in the control sample.

Concerning the liver esterase (Fig. 1), a total of 20 bands were identified. Out of these 20 bands, four bands (at Rf: 0.425, 0.45, 0.8 and 0.988) were absent in the control sample. Also, one esterase band (Rf= 0.1) was absent in two samples (3 and 4).

Table 2: Numbers of detected bands in each treatment for each animal sample

		1	2	3	4	ABF	SD
Serum	Est.	13	14	14	14	0.98	0.07
	Mdh	7	6	11	11	0.58	0.24
	Ldh	9	9	9	9	0.9	0.24
	Sod	7	5	7	6	0.69	0.37
Liver	Est.	16	20	19	19	0.93	0.14
	Mdh	8	8	8	8	0.88	0.25
	Ldh	3	3	3	3	1	0
	Sod	2	3	3	2	0.83	0.28
Kidney	Est.	17	17	18	17	0.86	0.24
	Mdh	3	3	3	3	1	0
	Ldh	5	5	5	5	1	0
	Sod	3	3	3	3	1	0
Spleen	Est.	8	9	10	10	0.93	0.12
	Mdh	1	1	1	1	1	0
	Ldh	6	6	5	6	0.95	0.1
	Sod	2	2	2	1	0.43	0.37

Est. = Esterase, Sod= Superoxide dismutase, Mdh = Malate dehydrogenase, Ldh = Lactate dehydrogenase, - = No detectable reaction, c= control, ta = first time, tb = second time, tc = third time and ABF = average of band frequencies SD= Standers deviation

A total of 20 esterase bands were characterized in the kidney (Fig. 1) tissue (Rf ranged from 0.05 to 0.738). One band was a control-specific esterase band (Rf= 0.188).

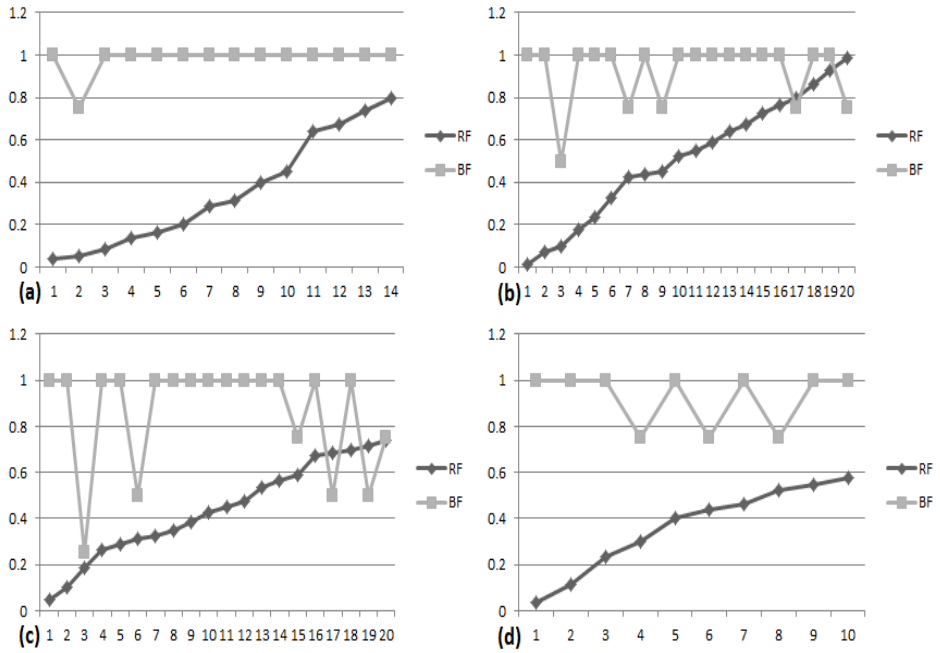

Fig. 2: Distribution of band frequencies (BF) and Relative fronts (RF) for each evaluated Esterase isozyme. Serum (a), Liver (b), Kidney (c) and Spleen (d) tissues

On the other hand, one band at the relative front 0.588 was absent in the control sample only. Also, two bands (at Rf 0.688 and 0.713) were absent in both the control and MTX samples. The results showed that the band at the Rf 0.738 was absent in the t4 sample.

Regarding the spleen (Fig. 1) tissue, the identified bands ranged from 8 to 10. The Rf ranged from 0.038 to 0.575. Two bands (Rf: 0.3 and 0.525) were absent in the control sample (S1). Also, band number 6 (Rf= 0.438) was absent in the MTX sample (Table 2).

The Relative fronts (RF) and distribution of the band frequencies (BF) of each evaluated Est isozymes in each evaluated tissue were presented in Fig. (2).

Malate dehydrogenase

The electrophoretic patterns of the Malate dehydrogenase (Mdh) isozymes (Fig. 3) in the four different samples (serum, liver, kidney and spleen) revealed notable bands.

The resolution and the total identified bands were summarized in Table (1). The averages of the band frequencies (ABF) were presented in Table (2).

A total of 15 serum Mdh bands (Fig. 3) were identified (the Rf ranged from 0.068 to 0.919). Only one serum Mdh band (Rf= 0.117) was specific for the control sample.

Concerning the liver Mdh, a total of 9 bands (Fig. 3) were identified (the Rf ranged from 0.133 to 0.881). Out of these bands, one band was absent from the control sample. On the other hand, this sample has a specific marker (band number 4) at the Rf 0.376.

A total of 3 common Mdh bands were identified in the kidney tissue extract (Rf ranged from 0.604 to 0.728). No variations were observed from the Kidney Mdh pattern.

Regarding the spleen tissue, only one band was identified (Rf: 0.66).

The Relative fronts (RF) and distribution of the band frequencies (BF) of each evaluated Mdh isozyme in each estimated tissue was presented in Fig. (4).

Lactate dehydrogenase

The electrophoretic patterns of the Lactate dehydrogenase (Ldh) isozymes (Fig. 5) in the different tissues revealed notable bands.

The resolution and the total identified bands were summarized in Table (1). The averages of the band frequencies (ABF) were presented in Table (2).

A total of 10 serum Ldh bands (Fig. 5) were identified (the Rf ranged from 0.13 to 0.93). Only one serum Ldh band (Rf= 0.13) was absent from the control sample.

Concerning the liver Ldh, a total of 3 bands were identified (the Rf ranged from 0.12 to 0.353). No variations were observed from the Kidney Ldh pattern.

A total of 5 common Ldh bands were identified in kidney tissue (Rf ranged from 0.174 to 0.754). No variations were revealed from the Kidney Ldh pattern.

Regarding the spleen (Fig. 5) tissue, a total of 6 bands were detected (the Rf ranged from 0.197 to 0.624). Only one band was absent from sample 3 (Rf: 0.624).

The Relative fronts (RF) and distribution of the band frequencies (BF) of each evaluated Ldh isozyme in each estimated tissue was presented in Fig. (6).

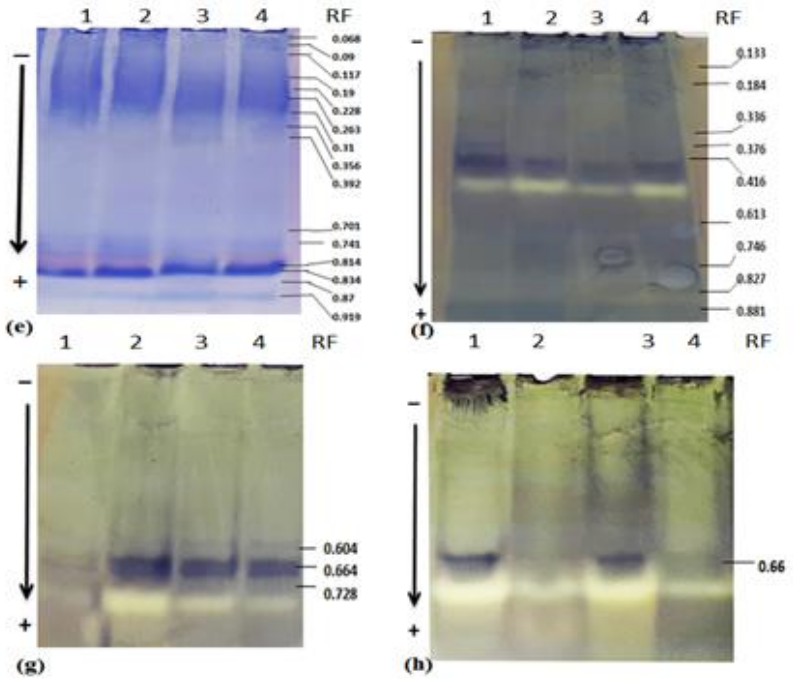

Fig. 3: The Malate dehydrogenase banding patterns from different samples. Serum (e), Liver (f), Kidney (g) and Spleen (h) tissues. 1= Control, 2= MTX, 3= MTX + ZnO-NPs and 4= ZnO-NPs

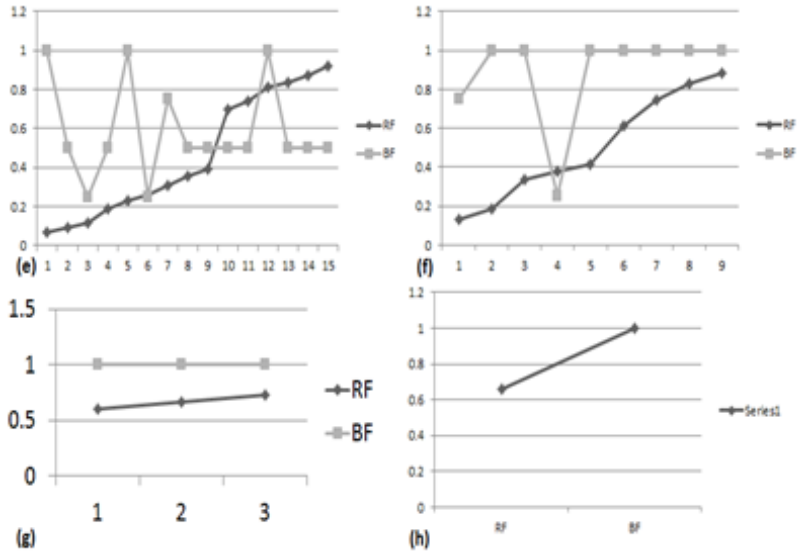

Fig. 4: Distribution of Band frequencies (BF) and Relative fronts (RF) for each evaluated Malate dehydrogenase isozyme. Serum (e), Liver (f), Kidney (g) and Spleen (h) tissues

Superoxide dismutase (SOD)

The electrophoretic patterns of the Lactate dehydrogenase (Sod) isozymes in the four different samples (serum, liver, kidney and spleen) were presented in Fig. (7).

The resolution and the total identified bands were summarized in Table (1). The averages of the band frequencies (ABF) were presented in Table (2).

A total of 9 serum Sod bands were identified (the Rf ranged from 0.154 to 0.931). A total of two serum Sod bands (Rf: 0.154 and 0.383) were specific for the control sample. Also, one marker (Rf= 0.397) was specific for sample number (3).

Concerning the liver Sod (Fig. 7), a total of 3 bands were identified (the Rf ranged from 0. 285 to 0.43). No variations were revealed from the Kidney Sod pattern (Fig. 7).

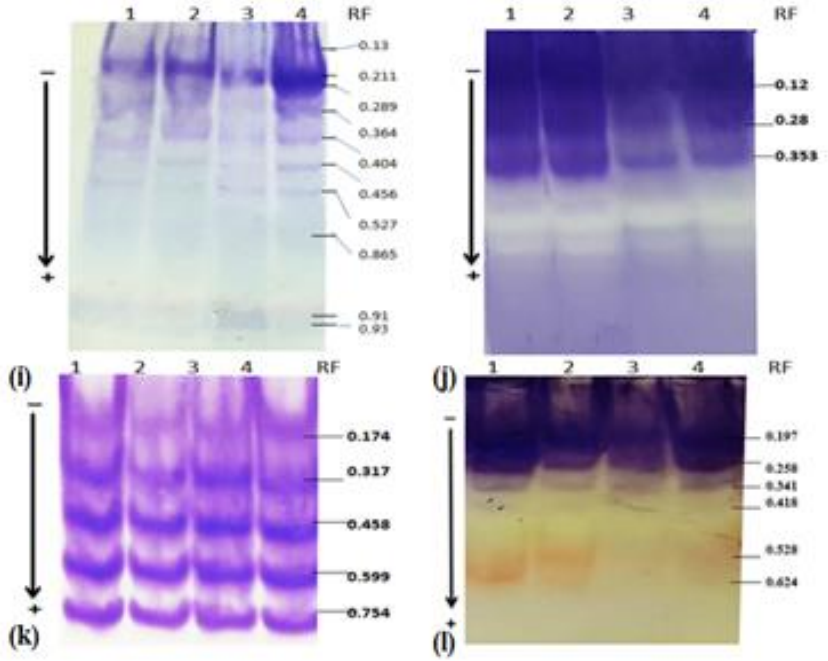

Fig. 5: The Lactate dehydrogenase banding patterns from different samples. Serum (i), Liver (j), Kidney (k) and Spleen (l) tissues. 1= Control, 2= MTX, 3= MTX + ZnO-NPs and 4= ZnO-NPs

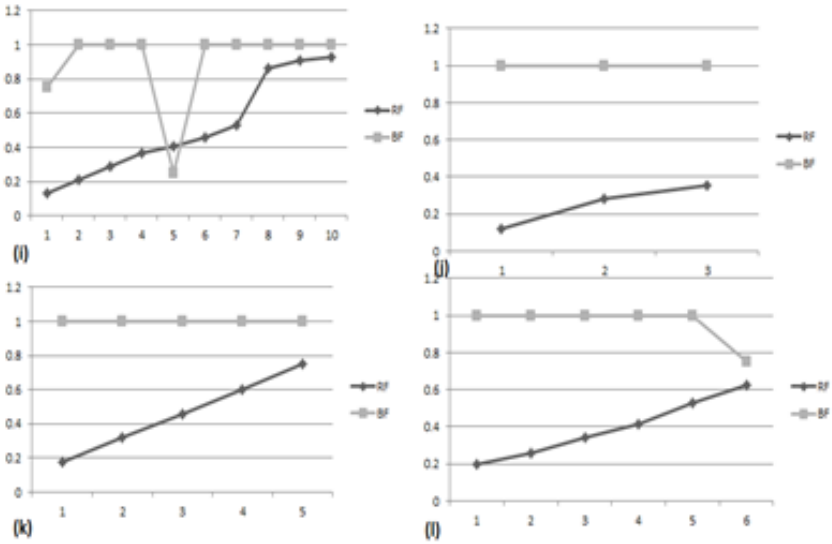

Fig. 6: Distribution of Band frequencies (BF) and Relative fronts (RF) for each evaluated Lactate dehydrogenase isozyme. Serum (i), Liver (j), Kidney (k) and Spleen (l) tissues

Regarding the spleen tissue, a total of four bands were detected (the Rf ranged from 0.694 to 0.94). Only one band was specific for the control sample (Rf: 0.711). Also, the bands at Rf 0.72 and 0.94 were specific for samples number 2 and 3 respectively.

The Relative fronts (RF) and distribution of the band frequencies (BF) of each evaluated Sod isozymes in each estimated tissue were presented in Fig. (8).

Analysis of liver SOD gene expression

To verify between the experimental and control individuals under the experimental conditions, a sqRT-PCR was applied to measure of the Sod gene expression in the liver tissues.

The result analysis indicated an up-regulation of liver Sod gene relative expression (Fig. 9) under the experimental

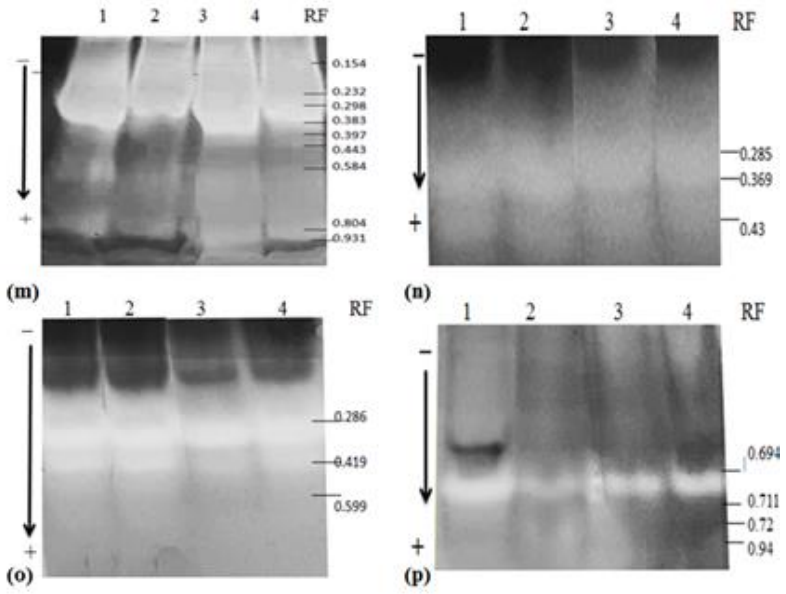

Fig. 7: The Superoxide dismutase banding patterns from different samples. Serum (m), Liver (n), Kidney (o) and Spleen (p) tissues. 1= Control, 2= MTX, 3= MTX + ZnO-NPs and 4= ZnO-NPs

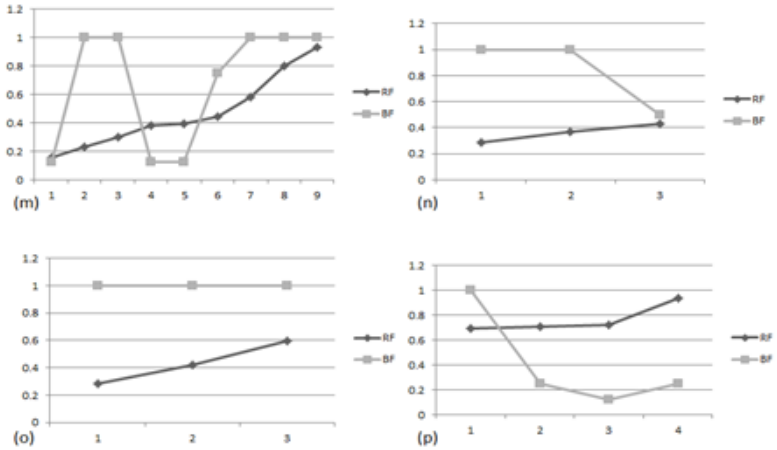

Fig. 8: Distribution of Band frequencies (BF) and Relative fronts (RF) for each evaluated Superoxide dismutase isozyme. Serum (m), Liver (n), Kidney (o) and Spleen (p) tissues

conditions in all treated samples, except for sample 2, which exhibited down-regulation, when compared to the control sample (1.28±0.001). There is a significant difference between sample medians ($p < 0.05$). The MTX treatment (treatment 2) exhibited the lowest relative expression (0.80±0.001) of Sod. Conversely, the ZnO-NPs treatment (treatment 4) demonstrated the highest relative expression (1.813±0.004) of Sod. The relative expression of Sod in the (MTX+ZnO-NPs (1.69±0.001) treatment (treatment 3) is higher than in the MTX treatment alone (treatment 2).

Discussion

The ZnO-NPs were prepared using the green method because the plant-derived nanoparticles are low-cost and eco-friendly to acquire when compared to nanoparticles derived from chemical and physical methods (Rahimi *et al*. 2022). Rahimi *et al*. (2022) recommended the estimation of various plant materials for the synthesis of ZnO-NPs for future investigations.

Some studies have examined the potential positive and/or negative effects of zinc oxide nanoparticles when administered orally (Pasupuleti *et al*. 2012; Mansouri *et al*. 2015; Muthuraman and Hwan 2015; Chen *et al.* 2020) but biochemical and/or molecular alteration due to exposure to such materials has not been sufficiently evaluated.

Sharma *et al*. (2012) found that sub-acute oral exposure to zinc oxide nanoparticles could induce oxidative stress and

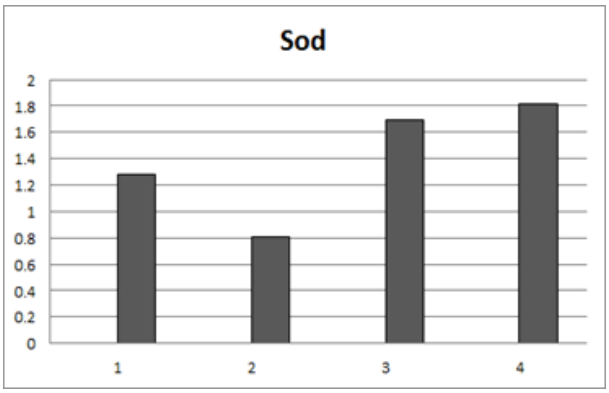

Fig. 9: Averages of the Gene expression of the Sod biomarkers in the liver. 1= Control samples (1.28±0.001), 2= MTX (0.80±0.001), 3= MTX+ZnO-NPs (1.69±0.001) and 4= ZnO-NPs (1.813±0.004). Values are mean ± SD. *$p < 0.05$, significantly different from control

apoptosis in the mouse liver. On the other hand, Fathi *et al.* (2016) found that when used as a feed supplement at a dosage of 20 mg/kg body weight in broilers, ZnO-NPs increased feed consumption and weight gain. Moreover, ZnO-NPs improved the antioxidant capacity in the birds by significantly increasing the serum concentrations of superoxide dismutase (SOD) and alkaline phosphatase (ALP) activities. Furthermore, the supplementation of ZnO-NPs led to elevated levels of high-density lipoprotein (HDL) and cholesterol in the serum. The results of the present study align with previous findings. We observed that the treatment involving ZnO-NPs exhibited the highest relative expression of Sod.

In a separate study conducted by Chen *et al.* (2020), it was discovered that exposure to zinc oxide nanoparticles resulted in fetal growth restriction and apoptosis in pregnant mice. Therefore, more investigations should be carried out for determining and evaluating the accurate effects of such nanoparticles on different organisms (at biochemical and/or molecular genetic levels.

Due to its sensitivity, isozyme electrophoresis (Alamri *et al*. 2021) and Semi-quantitative (Wang 2021) techniques were applied in the present study for detecting the effects of Zinc oxide nanoparticles and MTX on male mice body tissues including the liver, spleen and kidney. Also, these effects were evaluated on mice's serum.

The results showed that exposures to Zinc oxide nanoparticles and/or MTX can change the intensity and the numbers of some isozymes (Esterase, Malate dehydrogenase, Lactate dehydrogenase and Superoxide dismutase) in some body organs.

Isozyme systems have proven to be real tags of differential gene expression in various body organs. The results showed that the total numbers of some isozyme bands (kidney Mdh, spleen Mdh, liver Ldh and kidney Ldh) are not altered. On the other hand, the other tissue samples are affected by treatments under experimental conditions. These findings align with the observations of Mansour *et al*. (2012), who attributed the increased numbers and/or intensities of isozyme bands to the effects of Methotrexate (MTX) on mice. Also, both Alamri *et al*. (2021) and Elsebaie and Saad (2022) recommended these systems for developing informative biochemical tags for exploring the effects of various nanoparticles on different biological systems.

The cellular defense mechanisms against oxidative stress are supported by antioxidants such as superoxide dismutase, ascorbic acid, Metallothionein, and glutathione peroxidase. So, to verify between the experimental and control individuals under the experimental conditions, a Semiquantitative RT-PCR was applied to measure the Sod gene expression in the liver tissues. The samples were quantitatively measured to detect the utility of RNA extraction from the liver tissue and the percent validation of the mRNA to cDNA (Romero *et al.* 2007).

Concerning the sublethal concentration of ZnO-NPs, the expression of certain genes including in oxidative stress and apoptosis were increased (Esmaeillou *et al*. 2013; Rahimi *et al*. 2022). Also, some Rat thymus and spleen gene expressions were evaluated under certain ZnO-NPs treatments by Abass *et al*. (2017) via RT-PCR analysis. They observed the Upregulation of some immunomodulatory (like CD3) and inflammatory (like TLR4) genes. Abass *et al*. (2017) also estimated the effects of the ZnO-NPs (26.6±9.71nm) on the rat's thymus and spleen cell proliferation using biochemical and immunohistochemical analysis. The cellularity of the spleen and thymus and their structural integrity were affected by ZnO NPs. They found that exposure to ZnO-NPs triggered a decrease in serum TAC and an increase of MDA in both the spleen and thymus tissues. These results indicated that ZnO NPs initiated the oxide stress–ER stress actions. In addition, the apoptosis was enhanced. More molecular investigations are required to evaluate more gene expressions under various ZnO NPs treatments.

In the present study, data analysis showed upregulation of the liver Sod (antioxidants) gene expression under experimental conditions. Rahimi *et al.* (2022) confirmed that Zinc oxide nanoparticles prompted oxidative stress and upregulated the iNOS and TNF-α (inflammatory biomarkers) and suppressed the expression of Sod and CAT (antioxidant-related genes) in both mice liver and kidney tissues. On the other hand, Zinc oxide nanoparticles were not toxic at low concentrations while at high concentrations they could increase reactive oxygen species ROS (Syama *et al.* 2013).

Muthuraman and Hwan (2017) confirmed that the LDH, ALT, ALP and AST enzyme activities and mRNA expressions were significantly augmented in a dose-dependent mode. The cells are affected when exposed to a higher concentration of ROS.

The biological effects of Methotrexate are correlated to concentration and time-dependent. Al-Maruf *et al.* (2018) observed that the rat liver exposed to the MTX (300 µM) treatment prompted mitochondrial injury and cytochrome c

release. They concluded that MTX-induced cytotoxicity caused by reactive oxygen species formation and GSH oxidation leads to oxidative stress and mitochondrial injury in rat hepatocytes.

In the present study, the result analysis showed UP-Regulation of the liver Sod gene expression in all treatments except MTX (down regulation) compared with the control sample. This finding may be due to the experimental conditions especially the ZnO NPs concentration compared to the previous studies carried out by Rahimi *et al*. (2022) and Al-Maruf *et al*. (2018). So, we can confirm that the effects of both MTX and ZnO NPs on various gene expressions in certain mice body organs are affected by the material structure and concentrations.

Conclusion

The wide applications of nanoparticle technology hold a huge capacity for exploring its future fate in industry, agriculture and medicine (antimicrobial agents and anticancer Nano drugs). Exposures to Zinc oxide nanoparticles and/or MTX can alter the intensity and numbers of some isozymes in some body organs. Semiquantitative RT-PCR and Isozyme systems have proven to be real tags of differential gene expression in various body organs. The developed biochemical and/or molecular tags were informative by allowing the comparison among the evaluated samples. Also, the obtained results will be useful in understanding the physiological consequences of gene expression analysis. More biological tags could be developed to explore environmental health, especially in terms of environmental pollution ranks in future ecotoxicological research. To have a better understanding of effects induced by ZnO-NPs and/or MTX at the molecular level, the investigation of protein expression levels must be accompanied by transcriptomics and proteomics.

Acknowledgement

Authors cordially acknowledge to King Abdulaziz University and the conservation of biological aquatic resources research group (CBARRG), Biological Sciences Department, Faculty of Sciences, King Abdulaziz University for providing laboratory facilities with equipment and chemicals.

Author Contributions

Bakhsh, Noor, Saad Yasser Mohamed and Rabah, Samar planned the work, explained the results, made the write and made illustrations. Saeed, Mahmoud Ahmad statistically analyzed the data.

Conflict of Interest

The Authors declared no conflict of interest.

Data Availability

Data supporting the findings of this study are available from the corresponding author upon reasonable request

Ethics Approvals

This study was conducted in full accordance with ethical principles. All experimental protocols were carried out in accordance with the relevant guidelines and regulations

Funding Source

This study did not receive any specific grant from funding agencies in the public, commercial or not-for-profit sectors.

References

Abass M, S Selim, A Selim, A El-Shal, ZB Gouda (2017). Effect of orally administered zinc oxide nanoparticles on albino rat thymus and spleen. *Intl Union Biochem Mol Biol* 69:528–539

Adegbeye M, M Elghandour, A Barbabosa-Pliego, J Monroy, M Mellado, P Reddy, A Salem (2019). Nanoparticles in equine nutrition: Mechanism of action and application as feed additives. *J Equine Vet Sci* 78:29–37

Alamri RS, YM Saad, AM Majed, A Atef (2021). *Pterophyllum scalare* genome responses to silver nanoparticles. *Egypt J Aquat Biol Fish* 25:965–982

Al-Maruf A, PJ O'Brien, P Naserzadeh, R Fathian, A Salimi, J Pourahmad (2018). Methotrexate induced mitochondrial injury and cytochrome c release in rat liver hepatocytes. *Drug Chem Toxicol* 41:51–61

Cho W, R Duffin, F Thielbeer (2012). Zeta potential and solubility to toxic ions as mechanisms of lung inflammation caused by metal/metal oxide nanoparticles. *Toxicol Sci* 126:469–477

Chen B, W Hong, P Yang, Y Tang, Y Zhao, Z Aguilar, H Xu (2020). Nano zinc oxide induced fetal mice growth restriction, based on oxide stress and endoplasmic reticulum stress. *Nanomaterials* 10:259

Elsebaie HEA, YM Saad (2022). *Pomacea canaliculata* biological responses to silver nanoparticles. *Egypt J Chem* 65:1111–1120

Esmaeillou M, M Moharamnejad, R Hsankhani, A Tehrani, H Maadi (2013). Toxicity of ZnO nanoparticles in healthy adult mice. *Environ Toxicol Pharmacol* 35:67–71

Fathi M, M Haydari, T Tanha (2016). Effects of zinc oxide nanoparticles on antioxidant status, serum enzymes activities, biochemical parameters and performance in broiler chickens. *J Livestock Sci Technol* 4:7–13

Gojova A, B Guo, R Kota, J Rutledge, I Kennedy, A Barakat (2007). Induction of inflammation in vascular endothelial cells by metal oxide nanoparticles effect of particle composition. *Environ Health Perspect* 115:403–409

Hong H, F Wang, Y Zhang, S Graves, S Eddine, Y Yang, C Theuer, R Nickles, X Wang, W Cai (2015). Red fluorescent zinc oxide nanoparticle: A novel platform for cancer targeting. *ACS Appl Mater Interfaces* 7:3373–3381

Kumar S, P Venkateswarlu, V Rao, G Rao (2013) Synthesis, characterization and optical properties of zinc oxide nanoparticles. *Intl Nano Lett* 3:2–6

Lin W, Y Xu, C Huang, Y Ma, K Shannon, D Chen, H Yue-Wern (2009). Toxicity of Nano-and micro-sized ZnO particles in human lung epithelial cells. *J Nanoparticle Res* 11:25–39

Mansour A, M Salam, YM Saad (2012). Mice (*Mus musculus*) genome responses to methotrexate (MTX) and some plant extracts. *Life Sci J* 9:4881–4886

Mansouri E, L Khorsandi, M Orazizadeh, Z Jozi (2015). Dose-dependent hepatotoxicity effects of Zinc oxide nanoparticles. *Nanomed J* 2:273–282

Meadus WJ (2003). A Semi-Quantitative RT-PCR method to measure the in vivo effect of dietary conjugated linoleic acid on porcine muscle PPAR gene expression. *Biol Proced* 5:20–28

Muthuraman P, K Hwan (2017). ZnO nanoparticles augment ALT, AST, ALP and LDH expressions in C2C12 cells. *Saudi J Biol Sci* 22:679–684

Muthuraman P, K Hwan (2015). *In vitro* toxicity of zinc oxide nanoparticles. *Rev J Nanoparticle Res* 17:1–8

Pasupuleti S, S Alapati, S Ganapathy, G Anumolu, NR Pully, B Prakhya (2012). Toxicity of zinc oxide nanoparticles through oral route. *Toxicol Ind Health* 28:675–686

Pasteur N, G Pasteur, F Bonhomme, J Catalan, J Britton-Davidian (1988). *Practical Isozyme Genetics*, p:215. Ellis Horwood Limited, Chichester, England

Peters RJ, H Bouwmeester, S Gottardo, V Amenta, M Arena, M Arena, P Brandhoff, JPM Hans, A Mech, BM Filipa, QP Laia, H Rauscher, R Schoonjans, KU Anna, VV Maria, S Weigel, K Aschberger (2016). Nanomaterials for products and application in agriculture, feed and food. *Trends Food Sci Technol* 54:155–164

Rahimi G, KS Mohammad, M Zarei, M Shokoohi, E Oskoueian, MRM Poorbagher, E Karimi (2022). Zinc oxide nanoparticles synthesized using *Hyssopus Officinalis* L. Extract Induced oxidative stress and changes the expression of key genes involved in inflammatory and antioxidant systems. *Biol Res* 55:24

Rio D, M Ares, G Hannon, T Nilsen (2010). Purification of RNA using TRIzol (TRI reagent). *Cold Spring Harb Protoc* 6:5439

Romero M, M Grasa, M Esteve, J Fernández-López, M Alemany (2007). Semiquantitative RT-PCR measurement of gene expression in rat tissues including a correction for varying cell size and number. *Nutr Metab (Lond)* 4:26

Schmidt S, C Messner, C Gaiser, C Hämmerli, L Suter-Dick (2022). Methotrexate-induced liver injury is associated with oxidative stress, impaired mitochondrial respiration, and endoplasmic reticulum stress *in vitro*. *Intl J Mol Sci* 1:15116

Scherzad A, T Meyer, N Kleinsasser, S Hackenberg (2017). Molecular mechanisms of zinc oxide nanoparticle-induced genotoxicity. *Materials* 10:1427

Singh R, H Nalwa (2011). Medical applications of nanoparticles in biological imaging, cell labeling, antimicrobial agents, and anticancer nano drugs. *J Biomed Nanotechnol* 7:489–503

Singh P, SK Mishra, S Noel, S Sharma, SK Rath (2012). Acute exposure of apigenin induces hepatotoxicity in Swiss mice. *PLoS One* 7:e31964

Sharma V, P Singh, A Pandey, A Dhawan (2012). Induction of oxidative stress, DNA damage and apoptosis in mouse liver after sub-acute oral exposure to zinc oxide nanoparticles. *Mutation Res* 745:84–91

Syama S, S Reshma, P Sreekanth, H Varma, P Mohanan (2013). Effect of zinc oxide nanoparticles on cellular oxidative stress and antioxidant defense mechanisms in mouse liver. *Toxicol Environ Chem* 95:495–503

Wang F (2021). Semi-quantitative RT-PCR: An effective method to explore the regulation of gene transcription level affected by environmental pollutants. *Methods Mol Biol* 2326:95–103

Wei Z, X Lei, P Petersen, S Aja, G Wong (2014). Targeted deletion of C1q/TNF-related protein 9 increases food intake, decreases insulin sensitivity, and promotes hepatic steatosis in mice. *Amer J Physiol Endocrinol Metab* 306:E779–790

Wheeler D, R Vander-Griend, T Wronski, G Miller, E Keith, JE Graves (1995). The short- and long-term effects of methotrexate on the rat skeleton. *Bone* 16:215–221